Traffic jams induced by fluctuation of a leading car

Takashi Nagatani

Division of Thermal Science, Department of Mechanical Engineering, Shizuoka University, Hamamatsu 432-8561, Japan

We present a phase diagram of the different kinds of congested traffic triggered by fluctuation of a leading car in an open system without sources and sinks. Traffic states and density waves are investigated numerically by varying the amplitude of fluctuation using a car following model. The phase transitions among the free traffic, oscillatory congested traffic, and homogeneous congested traffic occur by fluctuation of a leading car. With increasing the amplitude of fluctuation, the transition between the free traffic and oscillatory traffic occurs at lower density and the transition between the homogeneous congested traffic and the oscillatory traffic occurs at higher density. The oscillatory congested traffic corresponds to the coexisting phase. Also, the moving localized clusters appear just above the transition lines.

PACS number(s): 05.90.+m, 47.35.+i, 89.40.+k

I. INTRODUCTION

Recently, traffic problems have attracted the interest of a community of physicists [1–3]. Traffic flow is a kind of many-body systems of strongly interacting cars. Recent studies reveal physical phenomena such as the nonlinear waves and nonequilibrium phase transitions [4–8]. When the car density increases, the jamming transition occurs and the traffic jams appear. The jamming transitions from the freely moving traffic to the jammed traffic have been studied by microscopic and macroscopic models [4–6,9–16]. The jamming transitions are very similar to the conventional phase transitions and critical phenomena: the freely moving traffic and jammed traffic correspond to the gas and liquid phases, respectively [8]. Furthermore, it has been shown that the metastability occurs near transition point and induces the hysteresis phenomenon [17]. In the coexisting phase where both the freely moving traffic and the jammed traffic can exist, the kink-antikink density wave appears. The density wave exhibits the typical properties of the nonlinear waves [18–21].

In many works, the jamming transitions and the density waves have been investigated for the system without any inhomogeneity and fluctuation (except for the randomness of the initial condition) under the periodic boundary condition. Very recently, using the continuum traffic models, Helbing, Hennecke, and Treiber [22] and Lee, Lee, and Kim [23] have studied the traffic flow with on-ramp under the open boundary condition. They have found that the different kinds of congested traffic are induced by variation of the inflow at the upstream freeway boundary and the ramp. It has been shown that there are such new additional dynamic phases as the moving localized clusters, pinned localized clusters, triggered stop- and-go traffic, and oscillatory congested traffic except for the conventional coexisting phases of the kink-antikink density wave traffic and homogeneous congested traffic. The inhomogeneity on ramp has the important effect on the freeway traffic under the open boundary. Nagatani has shown that the jamming transion between the oscillatory traffic and homogeneous congested traffic occurs on the neutral stability line for the traffic flow with a bottleneck under the periodic boundary condition [24].

The traffic flow on a one-lane highway is a unidirectionally interacting many particle system since a car interacts with one car ahead. When an downstream car changes the speed or headway, the variation propagate upstream. Then, it will die out or evolve to the density waves (traffic jams). Without fluctuation, the traffic flow is homogeneous over space under open boundary condition. However, when the velocity of a leading car fluctuates at a finite amplitude, the density waves may propagates upstream and the formation of the density waves will depend on the amplitude of fluctuation. The local dynamics of both closed and open systems is not different, and all perturbations propagate backward in a reference frame moving with the car velocity. Whenever the leading vehicle leads to local densities in the unstable region of the closed system, the traffic flow is also unstable in the open system. Until now, it is unknown whether fluctuation of a leading car induces the jamming transition in an open system without sources and sinks. It is important to know the phase diagram of this type of source-sinkless open system.

In this paper, we investigate the traffic jams induced by random fluctuation of a leading car under the open boundary condition without sources and sinks. We use the car following model of the microscopic models. We study the dynamic traffic states triggered by systematical variation of the amplitude of velocity fluctuation of a leading car. We show that there are the three distinct congested traffic: the moving localized clusters, the oscillatory congested traffic, and the homogeneous congested traffic. We present a phase diagram of the different kinds of congested traffic induced by velocity fluctuation of a leading car in the source-sinkless open system. We compare the phase diagram with that obtained under the periodic boundary condition.

II. MODEL

We consider many cars flowing on a one-lane highway without passing and inflow. Cars are numbered as $1,2,3,...,N,N+1,...$ from the last car upstream. It is supposed that the velocity of car N fluctuates randomly. Then, the fluctuation will propagate upstream. In time, it will die out or evolve to the density waves. We investigate the dynamic states of traffic and the criterion of appearance of density
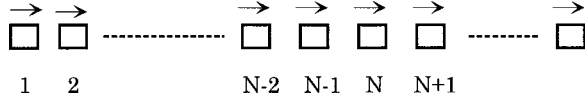
FIG. 1. Illustration of the traffic model. Cars are numbered as 1,2,3,...,N,$N+1$,..., from the last car. The velocity of car N fluctuates randomly.

waves. Figure 1 shows the schematic illustration of the traffic model. The dynamics of this system is essentially determined by the motion of the leading car, the so-called ahead long distance car. We use the car following model of the microscopic traffic models since it is difficult to take into account the fluctuation of a moving car in the continuum or macroscopic traffic models.

For later convenience, we summarize the car following models with the optimal velocity [5,8,20,25,26]. Newell [25] and Whitham [26] have analyzed the traffic model described by the following equation of motion of car j:

$$\frac{dx_j(t+\tau)}{dt} = V(\Delta x_j(t)), \qquad (1)$$

where $x_j(t)$ is the position of car j at time t, $\Delta x_j(t) = x_{j+1}(t) - x_j(t)$ is the headway of car j at time t, and τ is the delay time. The idea is that a driver adjusts the car velocity $dx_j(t)/dt$ according to the observed headway $\Delta x_j(t)$. The delay time τ allows for the time lag that it takes the car velocity to reach the optimal velocity $V(\Delta x_j(t))$ when the traffic flow is varying.

By Taylor expanding Eq. (1), one obtains the differential equation model [5]

$$\frac{d^2 x_j(t)}{dt^2} = a\left[V(\Delta x_j(t)) - \frac{dx_j(t)}{dt} \right], \qquad (2)$$

where a is the sensitivity of a driver [5] and $a = 1/\tau$. Furthermore, by transforming the time derivative to the difference in Eq. (1), one can obtain the difference equation model [20]

$$x_j(t+2\tau) = x_j(t+\tau) + \tau V(\Delta x_j(t)). \qquad (3)$$

Equation (3) is obtained only by assuming a forward difference approximation for the velocity, $dx_j(t+\tau)/dt = x_j(t+2\tau) - x_j(t+\tau)$. If one uses the symmetrical difference approximation $dx_j(t+\tau)/dt = x_j(t+2\tau) - x_j(t)$, the resulting difference equation does not exhibit traffic behavior similar to those of Eqs. (1) and (2).

The difference equation model is more suitable for computation since the time and space variables are discrete. The three models have been studied under the periodic boundary condition. It has been shown from simulation and analysis that the three models exhibit a similar traffic behavior and give a similar phase diagram [8,18,20]. The phase diagram of the difference equation model is shown in Fig. 2. The solid line indicates the coexisting curve. The dotted line indicates the spinodal line. The circle indicates the critical point. In each model, the traffic flow is divided into three regions: one is the stable region above the coexisting curve, the second is the metastable region between the spinodal line and the coexisting curve, and the third is the unstable region below the spinodal line. In the unstable region, the traffic
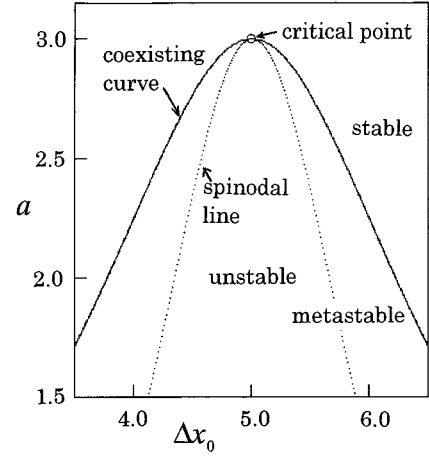

FIG. 2. Phase diagram of the difference equation model obtained from the linear and nonlinear analysis. The solid and dotted lines indicate, respectively, the coexisting and spinodal lines. The circle indicates the critical point.

jam appears as the kink-antikink density wave. The kink jam has been presented by the solution of the modified KdV equation. The densities out of and within the kink-antikink density wave are consistent with the densities on the coexisting curve under the constant value of a. Also, it has been shown that only near the neutral stability line (the spinodal line), the soliton density wave appears [27]. The soliton density wave has been described by the KdV equation.

Generally, it is necessary that the optimal velocity function has the following properties: it is a monotonically increasing function and it has an upper bound (maximal velocity). The optimal velocity function has been given by

$$V(\Delta x_j) = \frac{v_{\max}}{2}\{\tanh(\Delta x_j - h_c) + \tanh(h_c)\}, \qquad (4)$$

where h_c is the safety distance and $v_{\max}$ is the maximal velocity [5,8]. Equation (4) has the turning point (inflection point) at $\Delta x_j = h_c$:

$$V''(h_c) = \frac{d^2 V(\Delta x_j)}{d\Delta x_j^2}\bigg|_{\Delta x_j = h_c} = 0.$$

It is important that the optimal velocity function has the turning point. Otherwise, one cannot have the kink-antikink density wave solution representing the traffic jam.

The spinodal line has been obtained from the neutral stability condition [8,20]. It is given by

$$a = 1/\tau = 3V'(\Delta x_0), \qquad (5)$$

where Δx_0 is the average value of the headway and $V'(\Delta x_0)$ is the derivative of the optimal velocity function at Δx_0. The coexisting curve has been obtained from the solution of the modified KdV equation [8,20]. It is given by

$$\Delta x_0 = h_c \pm \sqrt{3\left(\frac{a_c}{a} - 1\right)} \quad \text{with} \quad a_c = 3v_{\max}/2. \qquad (6)$$
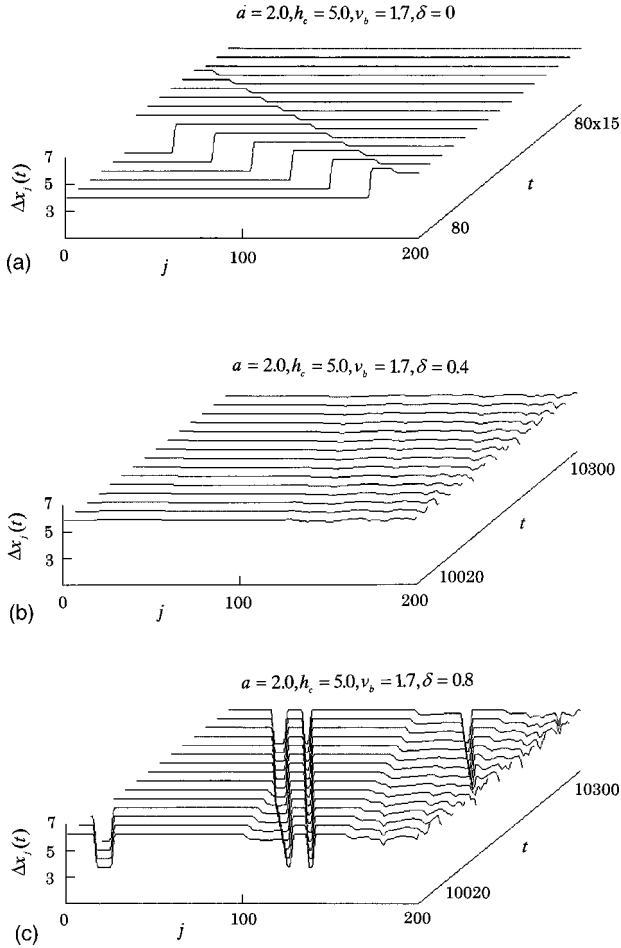
(a)

(b)

(c)

FIG. 3. Typical traffic patterns of headway. (a) The space-time evolution of headway without fluctuation at boundary for $\Delta x_0 = 4.0$ and $\nu_b = 1.7$. (b) The space-time evolution of headway with fluctuation from $t = 10\,020$ to $t = 10\,300$ at intervals of 20 time steps for $\nu_b = 1.7$ and $\delta = 0.4$. (c) The space-time evolution of headway with fluctuation from $t = 10\,020$ to $t = 10\,300$ at intervals of 20 time steps for $\nu_b = 1.7$ and $\delta = 0.8$. The density waves appear and propagate upstream.

The spinodal line and coexisting curve in Eqs. (5) and (6) are shown in Fig. 2 where $\nu_{\max} = 2.0$. The critical point is given by (h_c, a_c).

It is useful to rewrite Eq. (3) in terms of the headway. One obtains the following difference equation:

$$\Delta x_j(t + 2\tau) - \Delta x_j(t + \tau) - \tau\{V(\Delta x_{j+1}(t)) - V(\Delta x_j(t))\} = 0. \tag{7}$$

The boundary condition in this model is given by

$$\Delta x_{N-1}(t + \tau) = \Delta x_{N-1}(t) + \tau\{\nu_N(t) - V[\Delta x_{N-1}(t - \tau)]\},$$

with

$$\nu_N(t) = \nu_b + \delta[2\mathcal{R}(t) - 1.0] \tag{8}$$

where $\mathcal{R}(t)$ is the random number between zero and unity and ν_b is the average velocity of car N. The correlation is given by $\langle \mathcal{R}(t + m)\mathcal{R}(t)\rangle = \delta_{t+m,t}$ where $\delta_{t,t} = 1$ for $m = 0$ and $\delta_{t+m,t} = 0$ for $m \neq 0$. $\delta_{j,m}$ denotes the Kronecker delta. We note that the Kronecker delta is different from the am-
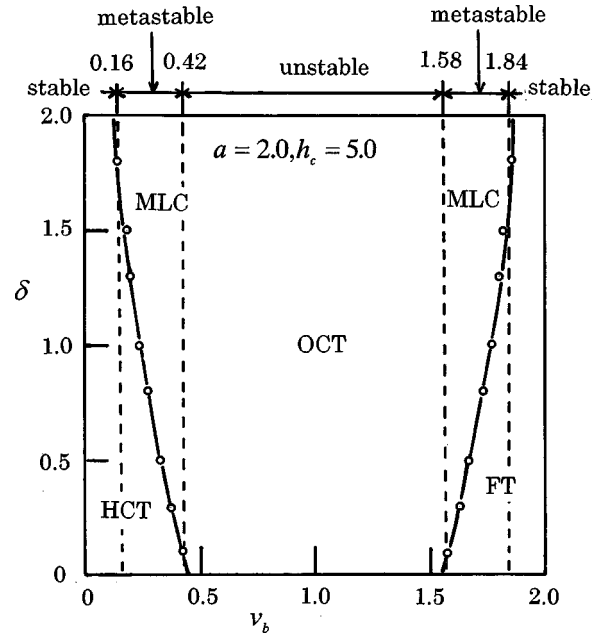

FIG. 4. Phase diagram of different kinds of the congested traffic triggered by fluctuation in (ν_b, δ) space where $a = 2.0$, $h_c = 5.0$. Displayed are the free traffic (FT), the moving localized clusters (MLC), the oscillatory traffic (OCT), and the homogeneous congested traffic (HCT).

plitude δ of fluctuation. Thus, the velocity of car N fluctuates randomly about the constant value ν_b with the amplitude δ.

III. SIMULATION

We carry out a computer simulation for the traffic flow described by Eqs. (7) and (8). We solve Eq. (7) by iteration under the boundary condition (8). We study the space-time evolution of headway for various values of amplitude δ. First, we study the case of $\delta = 0$ without fluctuation. We suppose that the headway is initially homogeneous over all cars: $\Delta x_j(0) = \Delta x_0$ and all cars move at the constant velocity given by $\nu_0 = V(\Delta x_0)$. In the steady state of the optimal velocity model, the velocity is uniquely related with the headway. The boundary condition is $\nu_N(t) = \nu_b$. In time, the traffic flow changes to the homogeneous state of $\Delta x_j(t) = V^{-1}(\nu_b)$, where V^{-1} is the inverse function of the optimal velocity. Figure 3(a) shows the space-time evolution of headway at intervals of 80 time steps for $\Delta x_0 = 4.0$ and $\nu_b = 1.7$ where $a = 2.0$, $h_c = 5.0$, and $N = 200$. Without fluctuation, the velocity of all upstream cars is a constant value of $\nu_b = 1.7$ uniquely determined by the boundary condition of car N. The headway of the homogeneous state is given by $\Delta x_j(t) = V^{-1}(1.7) =$ for $j = 1,2,\ldots,N-1$.

Secondly, we study the traffic flow in the metastable region with a finite amplitude of fluctuation. When the amplitude of fluctuation is small, the traffic flow is stable and nearly homogeneous over space except for fluctuation near the downstream boundary. Figure 3(b) shows the space-time evolution of headway from $t = 10020$ to $t = 10300$ at intervals of 20 time steps for $\nu_b = 1.7$ and $\delta = 0.4$ where $a = 2.0$, $h_c = 5.0$, and $N = 200$. When the amplitude is larger than the critical value, the density waves appear and propagate upstream. Figure 3(c) shows the space-time evolution of head-
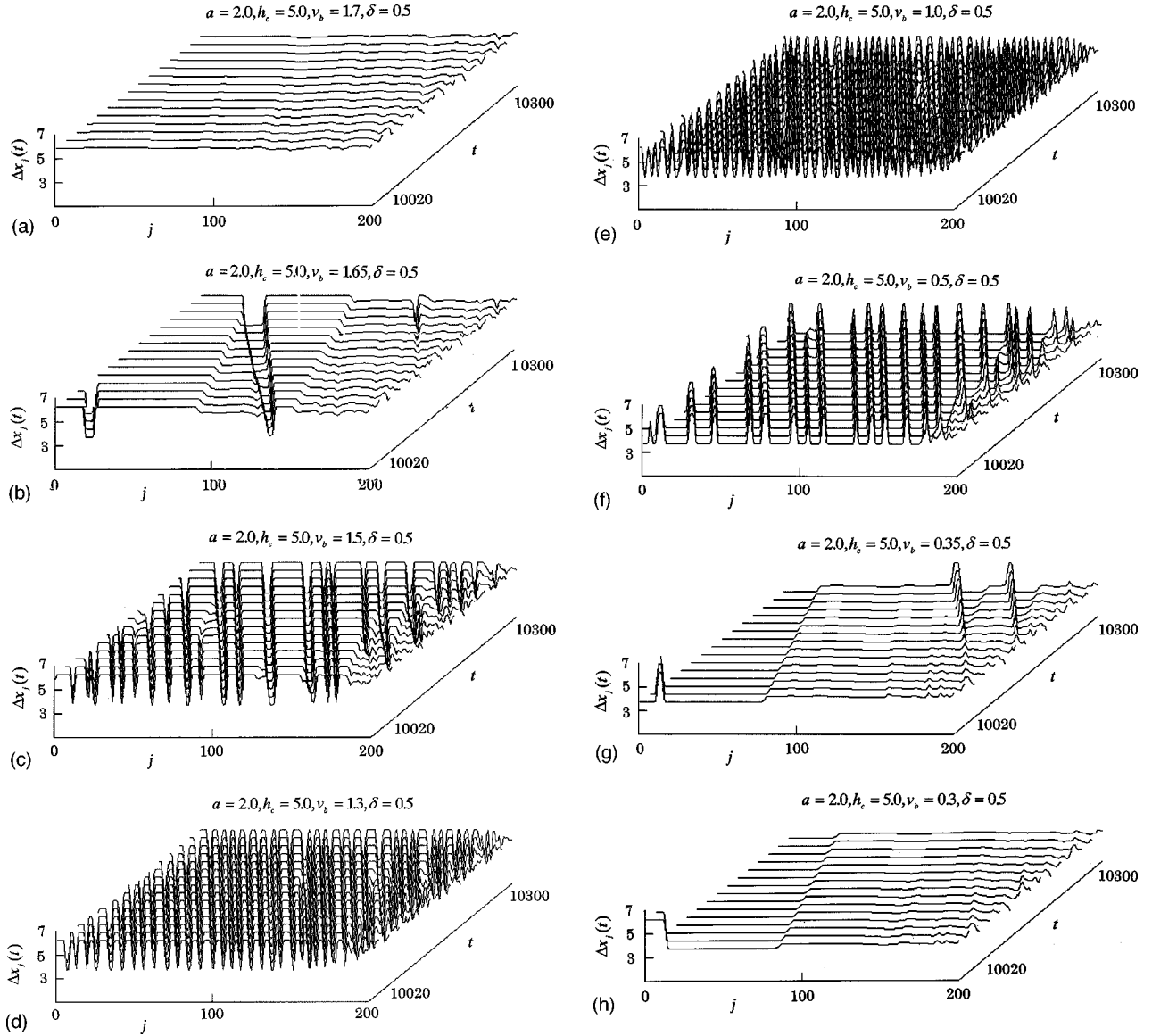
FIG. 5. Space-time evolutions of headway for the systematical variation of ν_b from $t = 10\,020$ to $t = 10\,300$ at intervals of 20 time steps for $a = 2.0$, $h_c = 5.0$, $\delta = 0.5$. (a) The free traffic for $\nu_b = 1.7$. (b) The moving localized clusters of the compression wave for $\nu_b = 1.65$. (c)–(f) The oscillatory traffic for $\nu_b = 1.5, 1.3, 1.0, 0.5$. (g) The moving localized clusters of the expansion wave for $\nu_b = 0.35$. (h) The homogeneous congested traffic for $\nu_b = 0.3$.

way from $t = 10020$ to $t = 10300$ at intervals of 20 time steps for $\nu_b = 1.7$ and $\delta = 0.8$ where $a = 2.0$, $h_c = 5.0$, and $N = 200$. The traffic flow is independent of the initial conditions for nonvanishing fluctuations. We use the initial condition of the homogeneous state with $\Delta x_j(0) = \Delta x_0 = \text{const}$.

We carry out the simulation by varying the amplitude δ and the velocity ν_b of the leading car. We obtain the phase diagram in (ν_b, δ) space where $a = 2.0, h_c = 5.0$. Figure 4 shows the phase diagram for $a = 2.0, h_c = 5.0$. The circles indicate the transition point between the homogeneous traffic and the traffic with density waves. The solid lines indicate the transition line connecting the transition points. The solid line on the right side represents the transition line between the free traffic (FT) and the congested traffic with density waves. The solid line on the left side represents the transition line between the homogeneous congested traffic (HCT) and the congested traffic with density waves. The two transition lines are symmetric against the line $\nu_b = V^{-1}(h_c) = 1.0$. The

two dotted lines on the right side of $\nu_b = V^{-1}(h_c) = 1.0$ indicate the neutral stability point (spinodal point) and the coexisting point. These points are given, respectively, by the values $\nu_b = V^{-1}(5.65) = 1.58$ and $\nu_b = V^{-1}(6.23) = 1.84$ for $a = 2.0, h_c = 5.0$. Similarly, the two dotted lines on the left side of $\nu_b = V^{-1}(h_c) = 1.0$ indicate the neutral stability point (spinodal point) and the coexisting point. These points are given, respectively, by the values $\nu_b = V^{-1}(4.35) = 0.42$ and $\nu_b = V^{-1}(3.77) = 0.16$ for $a = 2.0, h_c = 5.0$. The values are calculated by Eqs. (5) and (6). When Δx_b is within the unstable region between 4.35 and 5.65, the jammed traffic with density waves appears even if fluctuation is very weak. In the unstable traffic flow, the velocity is between $\nu_b = V^{-1}(5.65) = 1.58$ and $\nu_b = V^{-1}(4.35) = 0.42$. For weak fluctuation, the transition points agree with the neutral stability point obtained from the linear stability analysis [8,20]. With increasing the amplitude of fluctuation, the transition point between the free traffic (FT) and the density wave traf-
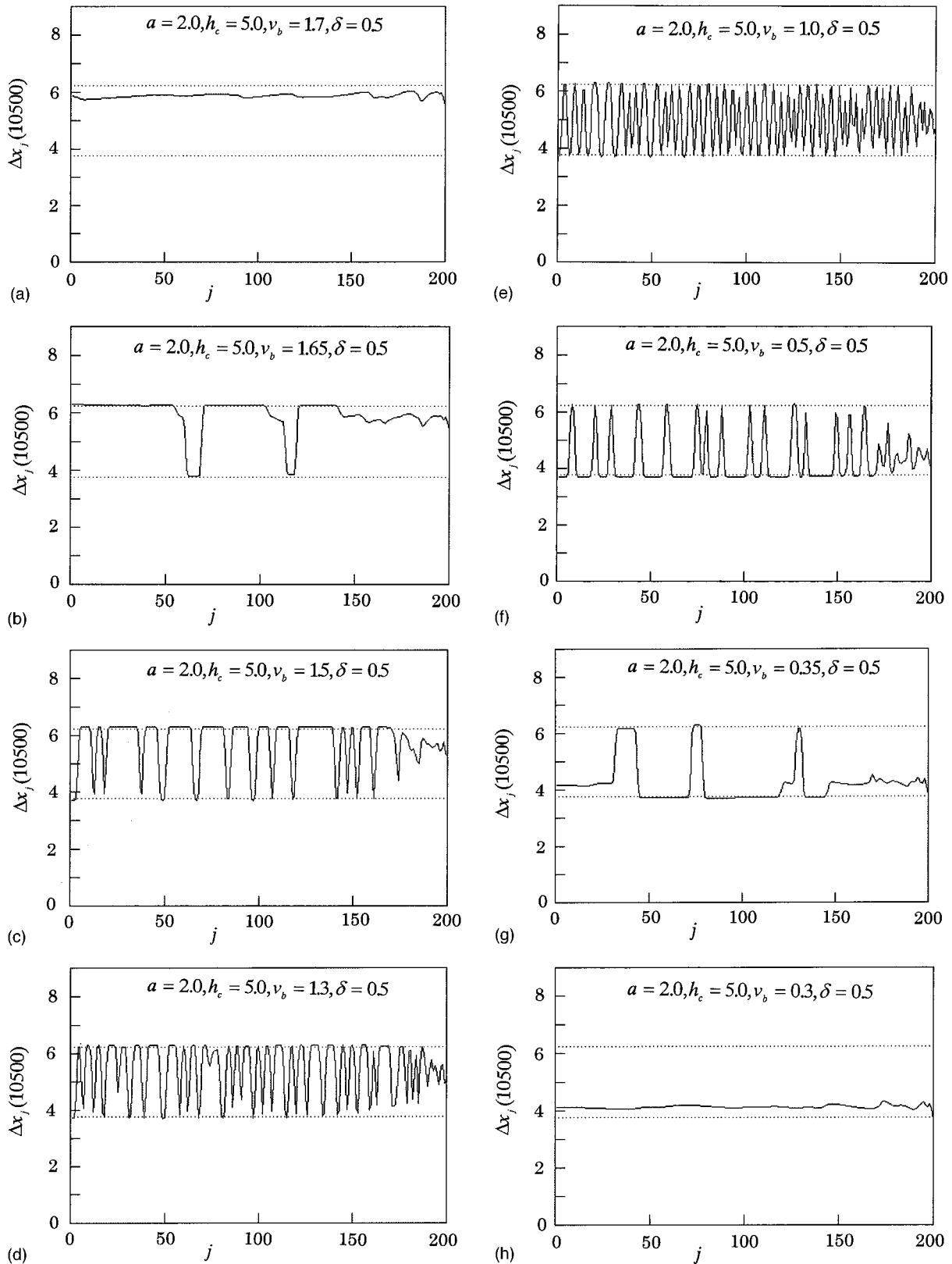
FIG. 6. Headway profiles at $t = 10\,500$ together with the coexisting points. The profiles (a)–(h) correspond to the space-time evolutions (a)–(h) in Fig. 5. The dotted lines indicate the coexisting points 3.77 and 6.23.

fic shifts to a larger value of velocity. Symmetrically, the transition point between the homogeneous congested traffic and the density wave traffic shifts to a lower value of velocity with increasing the amplitude of fluctuation. When the amplitude of fluctuation is large, the transition point approaches to the coexisting curve.

We study the traffic patterns induced by large amplitudes of fluctuation. We show the space-time evolution of headway for the systematical variation of boundary value v_b under $a = 2.0, h_c = 5.0, \delta = 0.5$. The patterns (a)–(h) in Fig. 5 exhibit

the space-time evolutions of headway, respectively, for ν_b = 1.7, 1.65, 1.5, 1.3, 1.0, 0.5, 0.35, 0.3 from t = 10020 to t = 10300 at intervals of 20 time steps. The value ν_b = 1.67 ± 0.02 of the first transition point between the free traffic and the density wave traffic is obtained, numerically, for δ = 0.5. The value ν_b = 0.33 ± 0.02 of the second transition point between the homogeneous congested traffic and the density wave traffic is obtained for δ = 0.5. The pattern (a) shows the free traffic before the transition. The headway profile is nearly homogeneous over space except for the neighborhood of the downstream boundary. The pattern (b) exhibits the moving localized clusters (MLC's) just after the transition. The traffic is the congested traffic with a single or a few density waves. The density wave is a compression wave and propagates backward. The traffic corresponds to the moving localized clusters found by Helbing *et al.* [22]. The patterns (c)–(f) show the oscillatory congested traffic (OCT). The number of density waves increases according as ν_b approaches to $\nu_c = V^{-1}(h_c) = 1.0$. The number reaches the maximum value at $\nu_c = V^{-1}(h_c) = 1.0$. Then, the number of density waves decreases according as ν_b departs from ν_c = 1.0. When ν_b is larger than ν_c = 1.0, the compression waves propagate backward as the density waves. When ν_b is less than ν_c = 1.0, the expansion waves propagate backward as the density waves. The pattern (g) exhibits the moving localized clusters just before the second transition. The traffic is the congested traffic with a single or a few density waves. The density wave is a expansion wave and propagates backward. The traffic corresponds to the moving localized clusters. The density wave of pattern (g) is not a compression wave but a expansion wave. This distinguishes pattern (g) from pattern (b). The MLC in the high density region is similar to that found in the macroscopic traffic flow model [28]. The pattern (h) exhibits the homogeneous congested traffic (OCT) after the second transition. The headway profile is nearly homogeneous over space except for the neighborhood of the downstream boundary. The pinned localized clusters are not found in the traffic jams triggered by fluctuation of a leading car. For comparing the headway with the coexisting points quantitatively, we show the headway profiles at t = 10500 together with the coexisting points. The profiles (a)–(h) in Fig. 6 exhibit, respectively, the plots of headway against car number j for ν_b = 1.7, 1.65, 1.5, 1.3, 1.0, 0.5, 0.35, 0.3. The profiles correspond to those at t = 10500 in the space-time evolution in Fig. 5. The dotted lines indicate the coexisting points 3.77 and 6.23 for a = 2.0, h_c = 5.0. The headway profile (a) is homogeneous over space except for the neighborhood of the downstream boundary. The value of headway is less than the value 6.23 at the coexisting point. The headway profile (h) is homogeneous over space except for the neighborhood of the downstream boundary. The value of headway is larger than the value 3.77 at the coexisting point. The compression density wave in the profile (b) has a kink-antikink form. The headways out of and

within the density wave agree, respectively, with the values 6.23 and 3.77 at coexisting points. Similarly, the expansion density wave in the profile (g) has a kink-antikink form. The headways out of and within the density wave agree with the values 3.77 and 6.23 at coexisting points. The strong density waves in the profiles (c)–(f) have the kink-antikink form. The headways out of and within the density wave agree with those at the coexisting points. Thus, the oscillatory traffic corresponds to the coexisting phase found in the periodic system. However, the jamming transition points induced by fluctuation are definitely different from those of the periodic system. The jamming transition depends strongly on the amplitude of fluctuation. The traffic jams induced by fluctuation are definitely different from the congested traffic triggered by the inhomogeneity.

We consider what happens if the fluctuation amplitude δ of the velocity of the leading car is larger than the average velocity ν_b. When $\delta > \nu_b$, the velocity $\nu_N(t)$ of the leading car becomes a negative value instantly. This means that the leading car moves averagely forward but moves instantly backward. This case occurs in Figs. 5(g), 5(h), 6(g), and 6(h). The backward moving of the car occurs seldom on a highway. However, the backward movement will be allowed in the theoretical model since the traffic models are closely related to the information traffic and the granular flow.

IV. SUMMARY

We have investigated the traffic jams triggered by velocity fluctuation of a leading car in an open system without sources and sinks by the use of the car following model. We have found the jamming transition triggered by the fluctuation of the leading car. We have shown that the jamming transition depends strongly on the amplitude of fluctuation. When the fluctuation is very small, the transition points are consistent with the neutral stability points predicted by the linear stability theory. When the amplitude of fluctuation is large, the jamming transition occurs in the metastable region. We have presented the phase diagram of the different kinds of congested traffic induced by fluctuation of the leading car. We have shown that the oscillatory traffic and moving localized clusters similar to those found in the different models appear in this model.

To our knowledge, this paper is the first work showing that fluctuation of a leading car induces the jamming transition in this new type of source-sinkless open system. There are at least three qualitatively different types of systems. (1) closed systems where the density or the average headway is the appropriate control parameter, (2) open systems with fixed boundaries and with vehicle sources and sinks where the traffic flux is the order parameter [29,30], and (3) source-sinkless open systems with moving boundaries which are described in this paper, where the velocity is the order parameter.

[1] *Traffic and Granular Flow*, edited by D. E. Wolf, M. Schreck-enberg, and A. Bachem (World Scientific, Singapore, 1996).

[2] D. Helbing, *Verkehrsdynamik* (Springer, Berlin, 1997).

[3] *Traffic and Granular Flow 97*, edited by M. Schreckenberg and D. E. Wolf (Springer, Singapore, 1998).

[4] K. Nagel and M. Schreckenberg, J. Phys. I **2**, 2221 (1992).

[5] M. Bando, K. Hasebe, A. Nakayama, A. Shibata, and Y. Sugiyama, Phys. Rev. E **51**, 1035 (1995).

[6] B. S. Kerner, P. Konhauser, and M. Schilke, Phys. Rev. E **51**, 6243 (1995).

[7] B. S. Kerner and H. Rehborn, Phys. Rev. E **53**, R1297 (1996).

[8] T. Nagatani, Phys. Rev. E **58**, 4271 (1998).

[9] O. Biham, A. A. Middleton, and D. A. Levine, Phys. Rev. A **46**, R6124 (1992).

[10] T. Nagatani, Phys. Rev. E **48**, 3290 (1993).

[11] J. A. Cuesta, F. C. Matinez, J. M. Nolera, and A. Sanchez, Phys. Rev. E **48**, 4175 (1993).

[12] K. Nagel, D. E. Wolf, P. Wagner, and P. Simon, Phys. Rev. E **58**, 1425 (1998).

[13] D. Helbing and M. Schreckenberg, Phys. Rev. E **59**, R2505 (1999).

[14] D. Helbing, Phys. Rev. E **53**, 2366 (1996).

[15] M. Treiber, A. Hennecke, and D. Helbing, Phys. Rev. E **59**, 239 (1999).

[16] K. Nagel, Phys. Rev. E **53**, 4655 (1996).

[17] S. Krauss, P. Wagner, and C. Gawron, Phys. Rev. E **55**, 5597 (1997).

[18] T. Komatsu and S. Sasa, Phys. Rev. E **52**, 5574 (1995).

[19] T. Nagatani and K. Nakanishi, Phys. Rev. E **57**, 6415 (1998).

[20] T. Nagatani, K. Nakanishi, and H. Emmerich, J. Phys. A **31**, 5431 (1998).

[21] T. Nagatani, Phys. Rev. E **59**, 4857 (1999).

[22] D. Helbing, A. Hennecke, and M. Treiber, Phys. Rev. Lett. **82**, 4360 (1999).

[23] H. Y. Lee, H. W. Lee, and D. Kim, Phys. Rev. E **59**, 5101 (1999).

[24] T. Nagatani, J. Phys. Soc. Jpn. **66**, 1928 (1997).

[25] G. F. Newell, Oper. Res. **9**, 209 (1961).

[26] G. B. Whitham, Proc. R. Soc. London, Ser. A **428**, 49 (1990).

[27] M. Muramatsu and T. Nagatani, Phys. Rev. E **60**, 180 (1999).

[28] B. S. Kerner, P. Konhauser, and M. Schilke, Phys. Lett. A **215**, 45 (1996).

[29] D. Helbing and M. Treiber, Phys. Rev. Lett. **81**, 3042 (1998).

[30] N. Mitarai and H. Nakanishi, J. Phys. Soc. Jpn. **68**, 2475 (1999).